

# Modulation of renal-specific oxidoreductase/*myo*-inositol oxygenase by high-glucose ambience

Baibaswata Nayak\*, Ping Xie\*, Shigeru Akagi\*, Qiwei Yang\*, Lin Sun\*, Jun Wada†, Arun Thakur\*, Farhad R. Danesh\*, Sumant S. Chugh\*, and Yashpal S. Kanwar\*<sup>‡§</sup>

Departments of \*Pathology and †Medicine, Northwestern University Medical School, Chicago, IL 60611; and ‡Third Department of Medicine, Okayama University, Okayama 700-8530, Japan

Communicated by Emanuel Margoliash, Northwestern University, Evanston, IL, October 18, 2005 (received for review August 31, 2005)

**Biological properties of renal-specific oxidoreductase (RSOR), characteristics of its promoter, and underlying mechanisms regulating its expression in diabetes were analyzed. RSOR expression, normally confined to the renal cortex, was markedly increased and extended into the outer medullary tubules in *db/db* mice, a model of type 2 diabetes. Exposure of LLCPK cells to  $D$ -glucose resulted in a dose-dependent increase in RSOR expression and its enzymatic activity. The latter was related to one of the glycolytic enzymes, *myo*-inositol oxygenase. The increase in activity was in proportion to serum glucose concentration. The RSOR expression also increased in cells treated with various organic osmolytes, e.g., sorbitol, myo-inositol, and glycerolphosphoryl-choline and  $H_2O_2$ . Basal promoter activity was confined to  $-1,252$  bp upstream of ATG, and it increased with the treatment of high glucose and osmolytes. EMSAs indicated an increased binding activity with osmotic-, carbohydrate-, and oxidant-response elements in cells treated with high glucose and was abolished by competitors. Supershifts, detected by anti-nuclear factor of activated T cells, and carbohydrate-response-element-binding protein established the binding specificity. Nuclear factor of activated T cells tonicity-enhancer-binding protein and carbohydrate-response-element-binding protein had increased nuclear expression in cells treated with high glucose. The activity of osmotic-response element exhibited a unique alternate binding pattern, as yet unreported in osmoregulatory genes. Data indicate that RSOR activity is modulated by diverse mechanisms, and it is endowed with dual properties to channel glucose intermediaries, characteristic of hepatic aldehyde reductases, and to maintain osmoregulation, a function of renal medullary genes, e.g., aldose reductase, in diabetes.**

diabetic nephropathy | hyperglycemia | osmoregulation

**D**iabetic nephropathy is characterized by hyperplasia/hypertrophy of intrinsic renal cells and increased extracellular matrices (1). These changes are related to the increased cellular flux of glucose intermediaries (2), *de novo* synthesis of intra- and extracellular advanced glycation end products (3, 4), activation of protein kinase C (5, 6), increased expression of transforming growth factor- $\beta$  (7), increased activity of GTP-binding and cell-cycle proteins (6, 8), and generation of reactive oxygen species (9, 10), with consequential compromise in renal functions (11, 12). Such complex interrelated cellular signaling events, also involving various forms of MAP/ERK kinases and Smad proteins, have been defined mainly in glomerular cells (13, 14); information relevant to the tubulointerstitial cells, although notably affected, is limited (15, 16). Conceivably, cellular changes in the tubulointerstitium parallel those in the glomerulus, with scarring and thickening of the basement membranes, and they correlate relatively better with the derangements in renal functional parameters (17, 18). Thus, much attention is warranted to the understanding of the pathophysiology of diabetic nephropathy with respect to tubular epithelial biology. A few years ago, we identified a renal tubular protein in mice with streptozotocin-induced diabetes by subtractive suppression hybridization-PCR, and the protein was designated as renal-specific oxidoreductase (RSOR) (19). RSOR is an  $\approx 32$ -kDa cytosolic

protein that is expressed in renal tubules and has an aldoketo reductase (AKR)-3 motif and an NADPH-binding site, as in aldose reductase (AR) and other AKR family members (20). Unlike other AKRs, the RSOR has a potential *N*-glycosylation site in the AKR-3 motif, suggesting complex structural characteristics and diverse regulatory functions. Interestingly, RSOR has an extensive homology with a glycolytic enzyme known as myo-inositol oxygenase (MIOX) (21) that catabolizes *myo*-inositol (MI) to  $D$ -glucuronate, which enters into the pentose phosphate pathway. The MI has a dynamic role for membrane phosphoinositides in providing for the release of second messengers, such as 1,2 diacylglycerol and inositol triphosphate; therefore, the RSOR, normally expressed in the cortex, conceivably modulates phosphoinositide signaling critical for various cellular events of the renal tubular epithelium. Another recently described gene, designated as kidney-specific protein-32 (*KSP32*), is also homologous to RSOR (22). The *KSP32* gene was discovered serendipitously in rats with acute renal failure. Nevertheless, it seems that RSOR may be largely relevant to glucose metabolism, in view of the original discovery made in the diabetic murine model (19) and the recent data suggesting its biphasic regulation in the kidneys of newborn mice with streptozotocin-induced diabetes (23). This communication describes the RSOR status in *db/db* mice, a genetic murine model of type 2 diabetes with certain lesions similar to those seen in man (24, 25), and the underlying mechanisms responsible for its gene regulation and MIOX activity.

## Materials and Methods

**Animals.** Six-week-old male diabetic *db/db* mice (*C57BLKS-lepr<sup>db</sup>/lepr<sup>db</sup>*) and control nondiabetic *db/m* (*C57BLKS/J-lepr<sup>db</sup>/+*) were obtained from The Jackson Laboratory, and CD1 mice, another control genetically unrelated strain, were purchased from Harlan. The mice were killed at 8, 12, and 16 wks of age, their kidneys were used for various studies, and blood was collected for glucose determination.

**Expression Studies.** Gene and protein expression of RSOR in mouse kidney and cells exposed to glucose and various osmolytes was carried out by Northern and Western blot analyses (19, 23). Spatiotemporal expression of RSOR in the kidneys was assessed by *in situ* hybridization and immunofluorescence microscopy (19, 23). In addition, expression of carbohydrate-response-element-binding protein (ChREBP) and nuclear factor of activated T cells (NFAT5)

Conflict of interest statement: No conflicts declared.

Abbreviations: AR, aldose reductase; ChRE, carbohydrate-response element; ChREBP, ChRE-binding protein; GPC, glycerolphosphorylcholine; MI, *myo*-inositol; MIOX, MI oxygenase; NFAT, nuclear factor of activated T cells; OsRE, osmotic-response element; OsREBP, OsRE-binding protein; OxRE, oxidant-response element; RSOR, renal-specific oxidoreductase; STRE, stress-response element.

<sup>§</sup>To whom correspondence should be addressed at: Department of Pathology, Northwestern University Medical School, 303 East Chicago Avenue, Chicago, IL 60611. E-mail: y-kanwar@northwestern.edu.

© 2005 by The National Academy of Sciences of the USA

in nuclear extract of cells treated with various osmolytes was carried out by immunoblot analyses.

**Enzyme Activity Analysis.** Kidney cortices were homogenized in a buffer containing 20 mM sodium acetate (pH 6.0), 2.0 mM L-cysteine, 1 mM ferrous ammonium sulfate, 1 mM glutathione, and 1 mM PMSF. The homogenate was centrifuged at  $20,000 \times g$  for 30 min, and the supernatant was saved, protein concentration adjusted to 10 mg/ml, and RSOR/MIOX activity measured (26). A typical 1-ml reaction mixture included 50 mM sodium acetate buffer (pH 6.0), 2.0 mM L-cysteine, 1 mM ferrous ammonium sulfate, 60 mM myoinositol, and 100  $\mu$ l of the supernatant. The reaction was carried out for 15 min at 30°C and terminated by the addition of 0.1 ml of 25% trichloroacetic acid. Precipitated protein was centrifuged, and the amount of D-glucuronic acid in the supernatant was determined.

**Cell Culture.** The renal proximal tubular epithelial cell line LLCPK was maintained in DMEM (GIBCO BRL) containing 5 mM D-glucose and 10% FBS. The concentration of FBS was reduced to 0.5% when the cells achieved  $\approx 80\%$  confluency for 12 h, and the cells were then treated with D-glucose for 48 h by adjusting its concentration in the medium to 5–50 mM. L-glucose served as control. Cells were also treated with various organic osmolytes, including polyols [(50 mM sorbitol, 50 mM mannitol, 1 mM *myo*-inositol, and 1 mM *chiro*-inositol) and tetramethylamines (100  $\mu$ M glycerophosphorylcholine (GPC) and 50 mM betaine] and 250 mM taurine. The cells were processed for expression studies and MIOX activity. Gene expression in cells treated with 20  $\mu$ M and 50  $\mu$ M of  $H_2O_2$  was assessed by RT-PCR (23). Cells were also processed for preparation of nuclear extract (27) for various EMSAs and expression of translocated transcription factors. Briefly, the nuclear pellet was resuspended in a half-packed nuclear volume of low-salt buffer [20 mM Hepes (pH 7.9)/1.5 mM  $MgCl_2$ /20 mM KCl/0.2 mM EDTA/25% glycerol (vol/vol)/0.5 mM DTT/0.5 mM PMSF]. An equal volume of high-salt buffer [20 mM Hepes (pH 7.9)/1.5 mM  $MgCl_2$ /800 mM KCl/0.2 mM EDTA/25% glycerol (vol/vol)/1% Nonidet P-40/0.5 mM DTT/0.5 mM PMSF/4.0  $\mu$ g/ml leupeptin, aprotinin, and pepstatin] was added. The nuclear suspension was gently shaken for 45 min at 4°C in an orbital shaker, followed by centrifugation at  $14,000 \times g$  for 15 min. The supernatant was collected and the protein concentration adjusted to 1 mg/ml.

**Isolation of 5' Flanking Region of RSOR Transcript and Generation of Reporter Constructs.** A DNA fragment of  $\approx 1.3$  kb flanking the 5' region was isolated from the mouse Ssp-I genomic library (Clontech) by using adapter AP-2 primer and a RSOR-specific antisense primer (5'-CACATCGACCTTCATCCTGAGGGAGC-3'). The DNA fragment was cloned in pCR 2.1 vector (Invitrogen) and used as a template for generation of serial-deletion PCR products by employing a common antisense primer 5'-GGGGGGGTACCTGAGGGAGCAGTCAC-3' and the following sense primers: 5'-GGGGGGGGTACCATGAGTTATCCCTT-3' (-1,252 to -1), 5'-GGGGGTACCCTTCTCTCTCCGAGGGTC-3' (-858 to -1), 5'-GGGGGTACCTATAGGGAGGGAAG ATTCTA-3' (-544 to -1), 5'-GGGGGTACCGGGTGGGTGAGGTCTGCCT-3' (-476 to -1), and 5'-GGGGGTACCCTGCTCTCTAGTGTGGCTC-3' (-338 to -1). A KpnI site, GG-TACC (underlined), was included in the primers. Another construct (-1,252 to -144) was generated by using the above -1,252-bp sense primer and another antisense primer, 5'-GGGGGGGTACCTCCTTCCTCCTGACCTC-3'. Products were cloned into pCR2.1 and subcloned into pGL3-basic vector (Promega). The inserts were sequenced and their orientation confirmed by using respective vector-specific sense (5'-CTAGCAAATAGGCTGTCCC-3') and antisense (5'-CTTTATGTTTTGGCGTCTTCCA-3') primers. The upstream 5' flank-

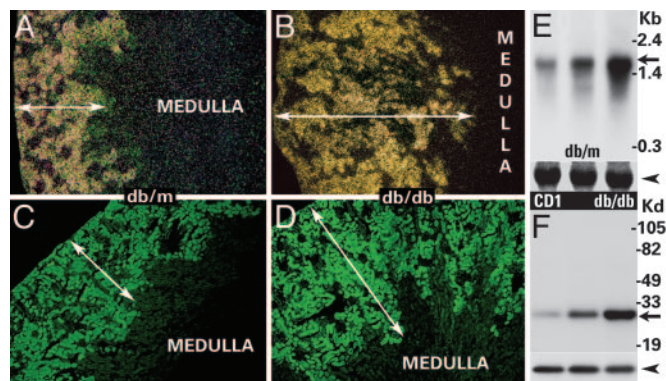


**Fig. 1.** Expression of RSOR in mice. *In situ* hybridization (A and B) and immunofluorescence (C and D) indicate RSOR localized to tubules of the outer renal cortex in CD1 or *db/m* mice (A and C,  $\leftrightarrow$ ). In *db/db* mice, the expression is markedly increased and extends into the medulla (B and D,  $\leftrightarrow$ ). (E and F) Northern and Western blots depicting RSOR expression (arrows) in CD1, *db/m*, and *db/db* mice at 16 wks. An increase in RSOR expression is seen in *db/db* mice, whereas  $\beta$ -actin (arrowheads) is unchanged.

ing sequence (up to  $\approx 3$  kb) of mouse RSOR and its homologues were retrieved from Ensembl bioinformatics ([www.ensembl.org](http://www.ensembl.org)). Transcription-factor-binding motifs and promoter prediction were searched at the following web sites: [www.motif.genome.ad.jp/MOTIF.html](http://www.motif.genome.ad.jp/MOTIF.html), [www.genomatix.de](http://www.genomatix.de), and <http://thr.cit.nih.gov/molbio/proscan>.

**Transfection of Cells and Luciferase Assays.** LLCPK1 ( $1 \times 10^6$  cells) were seeded onto 30-mm dishes in DMEM and maintained to achieve  $\approx 80\%$  confluency. Transfection was carried out by using 10  $\mu$ l of Lipofectamine (Life Technologies) and 3  $\mu$ g of reporter plasmid constructs. Cotransfection of 1  $\mu$ g of pcDNA-rLUC (renilla luciferase) was used as optimized equalization control. Assays for both renilla (rLUC) and firefly luciferase (LUC) activity were performed by using a Dual Luciferase kit (Promega). Basal promoter activity was determined in cells transfected with various reporter constructs and maintained in 5 mM glucose. To assess the effect of organic osmolytes on the promoter activity, the medium was replaced with opti-MEM (Invitrogen) containing various concentrations of osmolytes.

**EMSA.** Single-stranded sense and antisense oligonucleotides were synthesized, and their sequences are included in Table 1. Double-stranded annealed oligonucleotides were generated and end-labeled with  $\gamma P^{32}$ -ATP by using T4-polynucleotide kinase (Promega). Unlabeled oligonucleotides served as control. The binding reaction was carried out in a 20- $\mu$ l solution of binding buffer [50 mM Tris-HCl (pH 8.0)/750 mM KCl/2.5 mM EDTA/0.5% Triton X-100/62.5% glycerol (vol/vol)/1 mM DTT], 1–3  $\mu$ g/ $\mu$ l poly-[dI-dC], 1 pmol/ $\mu$ l probe, and 10  $\mu$ g of nuclear protein for 30 min at 24°C. For competition experiments, a 5- to 50-fold excess of cold unlabeled oligonucleotides was added. For supershift experiments, 1  $\mu$ g of antibody (anti-ChREBP and -NFAT5) was included in the reaction mixture and analyzed by 7.5% nondenaturing polyacrylamide gels, followed by autoradiography.

## Results

**RSOR Expression in *db/db* Mice.** *In situ* hybridization revealed the RSOR gene localized to outer renal cortical tubules at 8 wks of age in control animals (CD1 and *db/m*) and did not change up to 16 wks (Fig. 1A,  $\leftrightarrow$ ). In *db/db* mice, the expression was similar to controls, but it increased in its intensity and extended into the outer medulla by 16 wks (Fig. 1B,  $\leftrightarrow$ ). Comparable observations were made by immunofluorescence, where protein expression was confined to

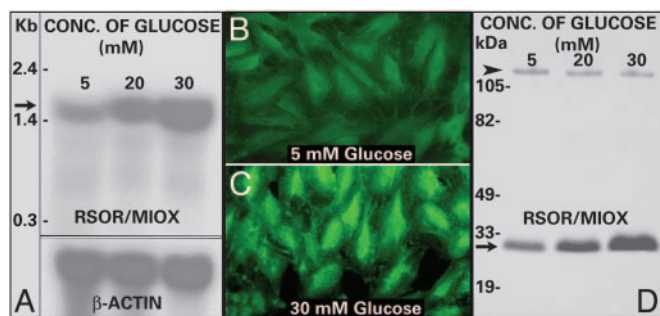


**Fig. 2.** RSOR expression in LLCPK cells treated with 5–30 mM D-glucose. Northern (A) and Western (D) blots indicate a dose-dependent increase in RSOR (arrows). The arrowhead in D represents a sample application site. (B and C) Increased *in situ* RSOR expression with 30 mM D-glucose.

cortical tubules (Fig. 1C,  $\leftrightarrow$ ), whereas, in *db/db* mice, it spanned into the outer medulla (Fig. 1D,  $\leftrightarrow$ ). Northern (Fig. 1E) and Western (Fig. 1F) blots indicated an increase in RSOR expression (arrows) in *db/db* mice compared with controls, although *db/m* mice had a higher expression than the genetically unrelated CD1 mice.

**RSOR Expression in LLCPK Cells.** A basal RSOR expression was observed in LLCPK cells cultured in DMEM containing 5 mM D-glucose. Northern (Fig. 2A) and Western (Fig. 2D) blots revealed a dose-dependent increased RSOR expression up to 30 mM D-glucose (arrows), with no further significant increase at 40 or 50 mM.  $\beta$ -actin expression was unchanged. Under high-glucose (30 mM) ambience, a marked increase in immunofluorescence was observed in cells stained with anti-RSOR antibody (Fig. 2C) compared with control (Fig. 2B).

**RSOR/MIOX Activity in Mouse Kidneys and LLCPK Cells.** Initially, the MIOX assay was standardized by using mouse recombinant RSOR. Basal enzyme activity in the kidneys of CD1 mice at 8 wks of age was designated as 100%, and the relative percent increase in various strains of mice is described (Fig. 3A). A mild increase in activity was observed with aging in CD1 and *db/m* mice. The *db/db* mice had a relatively high activity at 8 wks of age, and it increased remarkably at 12–16 wks. Accentuation in the RSOR/MIOX activity was proportional to the degree of hyperglycemia. Similarly, a dose-dependent increase in expression was also observed in cells treated with D-glucose (Fig. 3B).

**Isolation of 5' Flanking Region of Mouse RSOR and Promoter-Activity Analyses.** The highest basal promoter activity, defined as a relative luminescence unit (RLU) was observed when the whole intact

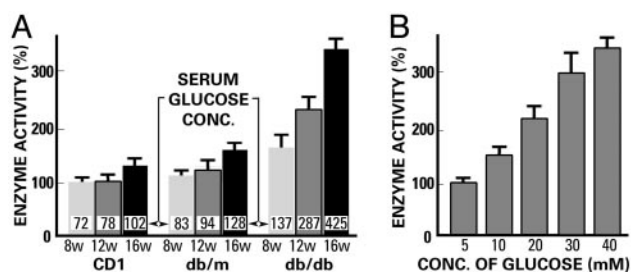


**Fig. 3.** RSOR/MIOX activity in kidneys and LLCPK cells. (A) Enzyme activity in CD1, *db/m*, and *db/db* mice at 8, 12, and 16 wks of age. An increase in activity is observed at 16 wks in *db/db* mice in proportion to serum glucose levels. A dose-dependent (5–40 mM) increase in enzyme activity is observed in cells treated with D-glucose (B). Basal activity in CD1 mice at 8 wks or cells treated with 5 mM D-glucose is designated as 100%. Data are derived from six animals or experiments.

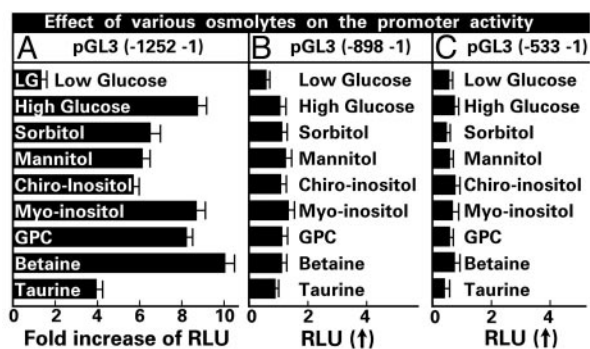


**Fig. 4.** Effect of osmolytes on RSOR promoter activity. Promoter activity was assessed by luciferase assay and expressed as relative luminescence units (RLU). (A) Data reflecting the effect of various osmolytes on the pGL3-1252 promoter activity, notably (8- to 10-fold) with the treatment of D-glucose, myo-inositol, GPC, and betaine. The other two deletion constructs, pGL3-898 and -544, had an only 1- to 2-fold increase in activity (B and C).

pGL3 -1,252-bp reporter construct was used (Fig. 4A). The remaining deletion constructs yielded variable basal promoter activity. Intriguingly, deletion of the -144-bp region flanking ATG drastically reduced activity. The -1,252-bp construct included GATA 1, 2, and 3 factors, CCAAT-enhancer-binding protein sequences, E-, GC-, and TATA-box motifs, and cap signals for transcription initiation. However, osmotic, carbohydrate- (glucose), stress-, and oxidant-response elements (OsRE, ChRE, STRE, and OxRE, respectively) were localized upstream of -600 bp (Table 1). By using this construct, a 5- to 10-fold increase in RLU was observed in cells exposed to high D-glucose (30 mM) and various organic osmolytes with different biological properties (Fig. 4B). The effect was especially notable with high glucose, *myo*-inositol, GPC, and betaine. The pGL3-898 and -544 exhibited an only 1- to 2-fold increase in RLU with the above treatments (Fig. 4C and D). Examination of a 3-kb upstream genomic sequence revealed several OsREs and ChREs and additional binding motifs, i.e., Sp1, AP1, upstream stimulating factor, and NFAT5, the latter two being involved in glucose metabolism and osmoregulation.

**Characterization of OsREs by EMSA.** NFAT5 is also known as OsRE-binding protein (OsREBP) or tonicity-responsive-enhancer-binding protein, with consensus sequence of binding motif as: NGGAAAWDHMN (the minimal OsRE motif is underlined) (28). Minimal GGAAA motif was present at six positions in the mouse RSOR 5' flanking sequence (Table 1). Oligonucleotides

**Table 1.** Oligomers used in electrophoretic mobility-shift assay

Element	Range	Sequence
OsRE-851	-861 to -832	<u>gccagtgtaggggaaacccctgtaagtatcaa*</u>
OsRE-1,239	-1,250 to -1,221	<u>ccctttataagggaaatcaaacacaacaaa</u>
OsRE-1,239 mutant		<u>ccctttataag-----aacacaacaaa</u>
OsRE-1,425	-1,437 to -1,408	<u>ctaaaccctctggaactaacagtggtggc</u>
OsRE-1,746	-1,756 to -1,727	<u>ttactaagtgggaaaataatgtttgtagg</u>
OsRE-2,029	-2,039 to -2,010	<u>gtcttaaaaagggaaaatatattgcccaggcag</u>
OsRE-2,622	-2,632 to -2,603	<u>tttaatgcaagggaaactgagctgaaggaaac</u>
ChRE-2,400	-2,405 to -2,346	<u>tgccctcagctgtaactca</u>
ChRE-1,063	-1,074 to -1,044	<u>gtttttcaagacacgggtttctctgtgtagc</u>
ChRE-1,063 mutant		<u>gtttttcaagacacgggtttctctgtgtagc</u>
Human ChRE	-1,380 to -1,345	<u>gagcagctgacactaccggtgttgggacacgtgagg</u>
AP1-1,442	-1,448 to -1,424	<u>ataatgaaatgactaaaacacctctgg</u>
Sp1-2,133	-2,136 to -2,114	<u>ccccccccccccccagagct</u>
STRE-659	-665 to -645	<u>gagggggcagggaggtctca</u>
OxRE-865	-865 to -843	<u>taaagccagtgagggaaccc</u>

\*The sequences are written as 5'-3' in sense orientation. The motifs are underlined, and mutations are in boldface type.



**Fig. 5.** Characterization of OsREs by EMSA. (A) Effect of osmolytes on binding activity of  $-1,239$ -bp OsRE oligonucleotide, seen as a shifted band (arrow). Lanes 1–9 show 5 mM D-glucose, 30 mM D-glucose, 50 mM sorbitol, 50 mM mannitol, 1 mM *chiro*-inositol, 1 mM *myo*-inositol, 0.1 mM GPC, 50 mM betaine, and 250 mM taurine. A supershift (SS) band (\*) is observed with anti-NFAT5 antibody in cells treated with 30 mM D-glucose (lane 10). (B) Dose-dependency with the treatment of D-glucose (5, 30, and 50 mM, lanes 1–3, respectively). Mutation of  $-1,239$ -bp OsRE oligonucleotide abolished the binding activity (C, lanes 1–3). (D) Data of alternate binding-activity pattern of various OsRE oligonucleotides, i.e.,  $-851$ ,  $-1,239$ ,  $-1,425$ ,  $-1,746$ ,  $-2,029$ , and  $-2,622$  bp (lanes 1–6). (E and F) Comparative binding data of OsRE-1,239 and -851 oligonucleotides in cells treated with 5 and 50 mM D-glucose (lanes 1 and 2) or 1 mM *myo*-inositol (lane 3), confirming alternate binding-activity pattern.

with this sequence were prepared and used for EMSA. A marked increase in the binding activity of tonicity-binding protein was observed with an oligonucleotide containing OsREs at the  $-1,239$ -bp position in cells treated with various osmolytes (Fig. 5A, lanes 2–9, arrow) compared with cells exposed to low 5 mM D-glucose (Fig. 5A, lane 1). The intensity of the shifted band was especially notable in cells treated with high D-glucose (30 mM), myoinositol, GPC, and betaine (Fig. 5A, lanes 2, 6, 7, and 8). The band supershifted to a higher position with anti-NFAT5 antibody included in the binding assay of cells treated with high glucose (Fig. 5A, lane 10). Binding was dose-dependent with increasing concentration of D-glucose (5–50 mM) (Fig. 5B, lanes 1–3). Deletion of motif GGAAA in the  $-1,239$  OsRE mutant abolished the binding activity (Fig. 5C), thus reinforcing the specificity of binding. Examination of all six OsREs, stretching from  $-851$  to  $-2622$  bp (Table 1), revealed that their binding activity is not uniform; rather, it occurs more efficiently at alternate positions, suggesting skipping during transcriptional activation by D-glucose (Fig. 5D, lanes 1, 3, and 5 vs. lanes 2, 4, and 6). This alternate binding-activity pattern is not exclusive to D-glucose (Fig. 5E vs. F, lanes 1 and 2) but is also observed with *myo*-inositol treatment (Fig. 5E and F, lanes 3), when the binding activities of OsREs at positions  $-1,239$  and  $-851$  bp were compared.

**Induction of Cytoplasmic RSOR and Nuclear NFAT5 in Cells Treated with Various Osmolytes.** Western blot analyses indicated that, compared with low 5 mM D-glucose, the cells exposed to various osmolytes had relatively high expression of RSOR (Fig. 6A), and, like the EMSA results (Fig. 5A, lanes 2–9), a markedly accentuated expression was seen with high 30 mM D-glucose, sorbitol, *myo*-inositol, and betaine (Fig. 6A, lanes 2, 3, 6, and 8). Concomitant with the up-regulation of RSOR, NFAT5 expression was also increased (Fig. 6C), suggesting a modulation of RSOR by the OsREBP, i.e., NFAT5.

**Characterization of Glucose/ChRE.** ChRE motifs conferring glucose/carbohydrate responsiveness are the repeat of two E boxes with consensus CACGGG/CCCGTG or palindromic CACGTG sequences with 5-bp spacing (29). Also, degenerate E-box motif sequences can also confer glucose responsiveness. In mouse RSOR, the CACGTG motif is present at  $-2,400$  bp. In its human homologue, the palindromic E-box motif (CACGTG) separated by 17 bp and a degenerate E-box motif (CCCGTG) motif with 5-bp spacing are present. Another putative ChRE motif CACGGT is present in

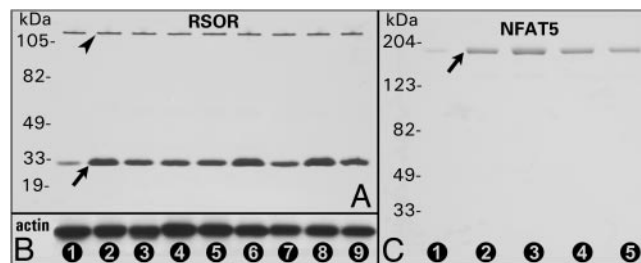


**Fig. 6.** Effect of osmolytes on RSOR and NFAT5 expression. (A) Western blot shows increased expression of RSOR (arrow) with the treatment of various osmolytes as described in Fig. 5 (lanes 1–9). A relatively high up-regulation of RSOR is seen with glucose, sorbitol, *myo*-inositol, and betaine treatment. The arrowhead represents a sample application site. The  $\beta$ -actin expression is unchanged (B). (C) Increased expression of tonicity-responsive-enhancer-binding protein (NFAT5,  $M_r \approx 170$  kDa) with the treatment of high glucose, sorbitol, mannitol, and *myo*-inositol (lanes 2–5, arrow) compared with control, 5 mM D-glucose (lane 1).

all species and was used for glucose responsiveness by EMSA (Table 1). When  $-2,400$  ChRE was used, a dose-dependent increase (5–50 mM D-glucose) in binding activity was observed (Fig. 7A, lanes 1–4, arrow). L-glucose treatment also yielded mild activity (Fig. 7B, lanes 1–4). With increasing concentration (5- to 10-fold) of competitor unlabeled probe, the binding efficiency was notably reduced (Fig. 7C), indicating the specificity of ChRE. Binding efficiency was almost identical in cells treated with the same concentration (50 mM) of D-glucose or sorbitol (Fig. 7D, lane 2 vs. lane 3), irrespective of the usage of  $-1,063$ -bp ChRE (Fig. 7E). Binding was completely abolished with a 50-fold excess of cold probe (Fig. 7D and E, lanes 4). Mutation in the  $-1,063$ -bp ChRE notably reduced the binding (Fig. 7F), conferring the functionality, in terms of glucose responsiveness, of the motif CACGGT. When the oligonucleotide stretching across E-box motifs was used, results almost similar to those of  $-2,400$ - or  $-1,063$ -bp ChRE were observed in cells treated with 50 mM D-glucose or sorbitol, although efficiency of binding was less (Fig. 7G vs. D/E, lanes 2 and 3). Nevertheless, binding was specific, because it was reduced by the competitor (Fig. 7G, lane 4), and a supershift was detected with anti-ChREBP antibody (Fig. 7G, lane 5). Moreover, like the up-regulation of RSOR and NFAT5 by organic osmolytes, an

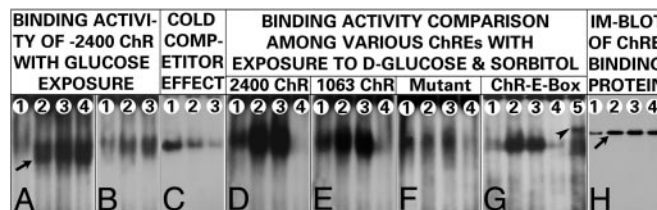


**Fig. 7.** Characterization of ChREs and E box by EMSA. (A) A dose-dependent (5, 15, 30, and 50 mM D-glucose, lanes 1–4, respectively) increase in binding (arrow) with  $-2,400$ -bp ChRE oligonucleotide. Mild binding is seen with 15, 30, and 50 mM L-glucose (B, lanes 1–3) and is reduced with a 5- to 10-fold excess of unlabeled oligonucleotide (C, lanes 2 and 3) compared with 30 mM D-glucose (lane 1). Comparative EMSA analyses (D and E) indicate that the  $-2,400$ -bp ChRE has a relatively higher binding activity than  $-1063$  ChRE in cells treated with 15 and 50 mM D-glucose and 50 mM sorbitol (D vs. E, lanes 1–3), which is abolished by a 50-fold-excess oligonucleotide (lane 4). Mutation of  $-1,063$  oligonucleotide reduced binding activity in cells treated with glucose and sorbitol (F, lanes 1–4). Analyses of the ChRE E box yielded similar binding activity, as seen in comparative studies (G, lanes 1–4), and the band supershifted to a higher position with anti-ChREBP antibody (lane 5, arrowhead). (H) Increased ChREBP protein ( $\approx 95$  kDa) expression (arrow) in cells treated with 50 mM D-glucose and sorbitol, and 1 mM *myo*-inositol (lanes 2–4) compared with control 5 mM D-glucose (lane 1).



that the binding was abolished with the competitor and the band supershifted to a higher molecular weight position (Fig. 7G, lanes 4 and 5) lends support to the theory that the ChREs and E box are relevant to the transcription of the *RSOR/MIOX* gene involved in the glycolytic pathway.

During glycolysis, the cell undergoes various forms of stresses, when subjected to high-glucose ambience with inductive transcription of a wide variety of genes (38). In addition to glycativ and osmotic stress, the oxidative stress related to reactive oxygen species has been well described in the literature (2, 9). Various elements relevant to stress-induced transcription include STRE, AP1, Sp1, OxRE, HNF-4, and upstream stimulating factor. STRE and OxRE are present in the 5' flanking region of *RSOR/MIOX*, in addition to AP1 and Sp1. The latter two have been described to be involved in the glucose-induced promoter activation of TGF- $\beta$ 1, a key cytokine responsible for evolution of glomerular lesions in diabetes (7). Consensus sequences for AP1 and Sp1 are also present in *RSOR/MIOX*, and the fact that a binding activity was detected by EMSA (Fig. 8 A–D) suggests that AP1 and Sp1 modulate the transcription of this enzyme and, thereby, the pathobiology of renal tubules. In regard to STRE, AP1 and Sp1 have been described in genes containing an E box responsive to hyperglycemia, e.g., *Uba52* (36), and these promoter elements also seem to be functional in this enzyme, as indicated by DNA–protein interactions (Fig. 8 E and F). The most interesting consensus elements identified in the *RSOR/MIOX* gene were OxREs relevant to oxidant stress, which is

believed to be the common denominator in diabetic pathobiology in target tissues (9). OxREs had a similar consensus sequence recently described in the bacterial *sufA* operon encoding iron–sulfur assembly proteins induced by superoxide generators and H<sub>2</sub>O<sub>2</sub> (30, 31). Our findings indicated that these OxREs are, indeed, operative in eukaryotic cells subjected to oxidative stress induced by D-glucose (Fig. 8 G and H). Moreover, H<sub>2</sub>O<sub>2</sub>-induced increased expression (Fig. 8I) would corroborate the data of D-glucose-induced up-regulation of *RSOR/MIOX*. Here, it is worth pointing out a potential paradox that a decreased *RSOR/MIOX* expression has been reported in acute renal failure (39), where tubular cells are under extreme oxidant stress (40). It may be that expression of the enzyme depends on the degree or type of oxidant stress (cytosolic vs. membrane vs. mitochondrial); nevertheless, it seems that OxREs are functionally active in *RSOR/MIOX* promoter.

In conclusion, *RSOR/MIOX* gene transcription is modulated by diverse elements localized within its promoter. Although localized in the renal cortex, *RSOR/MIOX* gene transcription is linked to the biology of osmoregulation, a function of genes expressed in the medulla, e.g., *AR*. Intriguingly, *RSOR/MIOX*, a *myo*-inositol-catabolizing cortical enzyme, undergoes an adaptive response to glucose challenge via ChRE elements described in the genes of hepatic enzymes regulating glycolysis/lipolysis.

This work was supported by National Institutes of Health Grants DK28492 and DK60635.

- Parving, H.-H., Osterby, R. & Ritz, E. (2000) *The Kidney*, ed. Brenner, B. M. (Saunders, Philadelphia), pp. 1731–1773.
- LeRoith, D., Taylor, S. I. & Olefsky, J. M. (2004) *Diabetes Mellitus: A Fundamental and Clinical Text* (Lippincott William & Wilkins, Philadelphia), 3rd Ed.
- Voziyan, P. A., Khalifah, R. G., Thibaudeau, C., Yildiz, A., Jacob, J., Seriani, A. S. & Hudson, B. G. (2003) *J. Biol. Chem.* **278**, 46616–46624.
- Jakus, V. & Rietbrock, N. (2004) *Physiol. Res.* **53**, 131–142.
- Whiteside, C. I. & Dlugosz, J. A. (2002) *Am. J. Physiol.* **282**, F975–F980.
- Lin, S., Sahai, A., Chugh, S. S., Pan, X., Wallner, E. I., Danesh, F. R., Lomasney, J. W. & Kanwar, Y. S. (2002) *J. Biol. Chem.* **277**, 41725–41735.
- Ziyadeh, F. N. (2004) *J. Am. Soc. Nephrol.* **15**, S55–S57.
- Danesh, F. R., Sadeghi, M. M., Amro, N., Phillips, C., Zeng, L., Lin, S., Sahai, A. & Kanwar, Y. S. (2002) *Proc. Natl. Acad. Sci. USA* **99**, 8301–8305.
- Brownlee, M. (2000) *Nature* **414**, 813–820.
- Schrauwen, P. & Hesselink, M. K. (2004) *Diabetes* **53**, 1412–1417.
- Kashihara, N., Watanabe, Y., Makino, H., Wallner, E. I. & Kanwar, Y. S. (1992) *Proc. Natl. Acad. Sci. USA* **89**, 6309–6313.
- Mason, R. M. & Wahab, N. A. (2003) *J. Am. Soc. Nephrol.* **14**, 1358–1373.
- Yang, Y. C., Piek, E., Zavadil, J., Liang, D., Xie, D., Heyer, J., Pavlidis, P., Kucherlapati, R., Roberts, A. B. & Bottinger, E. P. (2003) *Proc. Natl. Acad. Sci. USA* **100**, 10269–10274.
- Runyan, C. E., Schnaper, H. W. & Poncelet, A. C. (2005) *J. Biol. Chem.* **280**, 8300–8308.
- Ziyadeh, F. N., Simmons, D. A., Snipes, E. R. & Goldfarb, S. (1991) *J. Am. Soc. Nephrol.* **1**, 1220–1229.
- Phillips, A. O. (2003) *Curr. Diabetes Rep.* **3**, 491–496.
- Nath, K. A. (1998) *Kidney Int.* **54**, 992–994.
- Nath, K. A. (1992) *Am. J. Kidney Dis.* **20**, 1–17.
- Yang, Q., Dixit, B., Wada, J., Tian, Y., Wallner, E. I., Srivastava, S. K. & Kanwar, Y. S. (2000) *Proc. Natl. Acad. Sci. USA* **97**, 9896–9901.
- Hyndman, D., Bauman, D. R., Heredia, V. V. & Penning, T. M. (2003) *Chem. Biol. Interact.* **143**, 621–631.
- Arner, R. J., Prabhu, K. S., Thompson, J. T., Hildenbrandt, G. R., Linken, A. D. & Reddy, C. C. (2001) *Biochem. J.* **300**, 313–320.
- Hu, E., Chen, Z., Fredrickson, T., Gellai, M., Jugus, M., Contino, L., Spurr, N., Sims, M., Halsey, W., Van Horn, S., Mao, J., Sathe, G. & Brooks, D. (2000) *Am. J. Physiol.* **279**, F426–F439.
- Kanwar, Y. S., Akagi, S., Nayak, B., Lin, S., Wada, J., Xie, P., Thakur, A., Chugh, S. S. & Danesh, F. R. (2005) *Kidney Int.* **68**, 1670–1683.
- Cohen, M. P., Clements, R. S., Hud, E., Cohen, J. A. & Ziyadeh, F. N. (1996) *Exp. Nephrol.* **4**, 166–171.
- Sharma, K., McCue, P. & Dunn, S. R. (2003) *Am. J. Physiol.* **284**, F1138–F1144.
- Charalampous, F. C. & Lyras, C. (1957) *J. Biol. Chem.* **228**, 1–13.
- Dignam, J. D., Lebovitz, R. M. & Roeder, R. G. (1983) *Nucleic Acids Res.* **11**, 1475–1489.
- Go, W. Y., Liu, X., Roti, M. A., Liu, F. & Ho, S. N. (2004) *Proc. Natl. Acad. Sci. USA* **101**, 10673–10678.
- Ishii, S., Iizuka, K., Miller, B. C. & Uyeda, K. (2004) *Proc. Natl. Acad. Sci. USA* **101**, 15597–15602.
- Lee, J.-H., Yeo, W.-S. & Roe, J.-H. (2004) *Mol. Microbiol.* **51**, 1745–1755.
- Goldsmith-Fischman, S., Kuzin, A., Edstrom, W., Benach, J., Shastry, R., Xiao, R., Acton, T., Honig, B., Montelione, G. & Hunt, J. F. (2004) *J. Mol. Biol.* **344**, 549–565.
- Ziyadeh, F. N. (1996) *Kidney Int.* **54**, S10–S13.
- Burg, M. (1995) *Am. J. Physiol.* **268**, F983–F996.
- Kawa, J. M., Przybylaski, R. & Taylor, C. G. (2003) *Exp. Biol. Med.* **228**, 907–914.
- Yamashita, H., Takenoshita, M., Sakurai, M., Bruick, R. K., Henzel, W. J., Shillinglaw, W., Arnot, D. & Uyeda, K. (2001) *Proc. Natl. Acad. Sci. USA* **98**, 9116–9121.
- Sun, L., Pan, X., Wada, J., Haas, C. S., Wuthrich, R. P., Danesh, F. R., Chugh, S. S. & Kanwar, Y. S. (2002) *J. Biol. Chem.* **277**, 29953–29962.
- Zhu, Y., Casado, M., Vaulont, S. & Sharma, K. (2005) *Diabetes* **54**, 1976–1984.
- Vaulont, S., Cognet, V. M. & Kahn, A. (2000) *J. Biol. Chem.* **275**, 31555–31558.
- Hu, E., Chen, Z., Fredrickson, T., Gellai, M., Jugus, M., Contino, L., Spurr, N., Van Horn, S., Mao, J., Sathe, G. & Brooks, D. (2000) *Am. J. Physiol.* **279**, F426–F439.
- Nath, K. A. & Norby, S. M. (2000) *Am. J. Med.* **109**, 665–678.